7-Nitrobenz-2-oxa-1,3-diazole-4-yl-Labeled Phospholipids in Lipid Membranes: Differences in Fluorescence Behavior

Serge Mazères, Vincent Schram, Jean-François Tocanne, and André Lopez
Laboratoire de Pharmacologie et Toxicologie Fondamentales du CNRS, Department III, 31062 Toulouse, France

ABSTRACT Steady-state and time-resolved fluorescence properties of the 7-nitrobenz-2-oxa-1,3-diazole-4-yl (NBD) fluorophore attached either to the sn-2 acyl chain of various phospholipids (phosphatidylcholine, phosphatidylethanolamine, phosphatidylserine, and phosphatidic acid) or to the polar headgroup of phosphatidylethanolamine were studied after insertion of these NBD-labeled lipid probes into unilamellar vesicles of phosphatidylcholine, phosphatidylglycerol, phosphatidic acid, and phosphatidylserine. The fluorescence response of the NBD group was observed to strongly depend on the chemical structure and physical state of the host phospholipids and on the chemical structure of the lipid probe itself. Among the various fluorescence parameters studied, i.e., Stokes' shifts, lifetimes, and quantum yields, the quantum yields were by far the most affected by these structural and environmental factors, whereas the Stokes' shifts were practically unaffected. Thus, depending on the phospholipid probe and the host phospholipid, the fluorescence emission of the NBD group was found to vary by a factor of up to 5. Careful analysis of the data shows that for the various couples of probe and host lipid molecules studied, deexcitation of the fluorophore was dominated by nonradiative deactivation processes. This great sensitivity of the NBD group to environmental factors originates from its well-known solvatochromic properties, and comparison of these k_{nr} values with those obtained for *n*-propylamino-NBD in a set of organic solvents covering a large scale of polarity indicates that in phospholipids, the NBD fluorophore experiences a dielectric constant of around 27–41, corresponding to a medium of relatively high polarity. From these ϵ values and on the basis of models of the dielectric transition that characterizes any water-phospholipid interface, it can be inferred that for all of the phospholipid probes and host phospholipids tested, the NBD group is located in the region of the polar headgroups, near the phosphoglycerol moiety of the lipids.

INTRODUCTION

Since its introduction in 1968 (Ghosh and Whitehouse, 1968), the 7-nitrobenz-2-oxa-1,3-diazole-4-yl (NBD) group has been increasingly used as a fluorophore (Chattopadhyay, 1990). It displays the interesting property of fluorescing weakly in water and strongly in organic solvents, membranes, or hydrophobic environments. Its applications encompass wide areas of interest, and it is particularly interesting because its chloride and fluoride derivatives react easily with thiol or amino groups, leading to stable fluorescent adducts, which means that the NBD group may be used for labeling biological substrates. In membranology, various phospholipids and cholesterol analogs have been synthesized with the NBD group attached either to the polar headgroup or to the nonpolar fatty acyl chain of the lipids (Chattopadhyay, 1990). These lipid probes have been used for studying membrane phase transitions (Ellens et al., 1986; Hong et al., 1988), membrane fusion (Stuck et al., 1981), lipid sorting in polarized cells (Bacallao et al., 1989), intracellular lipid transport and lipid metabolism in living cells (Pagano and Sleight, 1985), aminophospholipid translocase activity (Pagano and Martin, 1988; Devaux, 1991; Julien et al., 1993), lipid lateral diffusion (Schram et al., 1994; Tocanne et al., 1994), and lipid domains (Julien et al., 1993; Welti and Glaser, 1994; Edidin, 1993).

The validity of the lipid probe approach in the study of membranes relies on various factors. In particular, the lipid probe must be as similar as possible to the native lipids. The probe location must be well defined in depth within the membrane, the probe must be randomly distributed within the host lipids, and the changes of the probe response with the microenvironmental polarity must be determined.

The possibility of labeling the polar headgroups or the acyl chains of phospholipids covers the first point. With respect to its location, fluorescence quenching studies in model membranes have shown that in phosphatidylcholine, the NBD group stays preferentially in the polar headgroup/hydrocarbon region, both for lipids labeled on the polar head like N-NBD-PE and for lipids labeled at the end of the sn-2 acyl chain like NBD(C_{12})-PC (Chattopadhyay and London, 1987, 1988; Abrams and London, 1993). In the latter case, looping back of the fluorophore to the membrane surface occurs, probably because of the polarity of the NBD group and the flexibility of the acyl chain to which it is attached.

Miscibility properties of NBD-labeled lipids have not been systematically investigated. However, from most of the studies carried out so far, one can conclude that at low concentrations (less than a few mole% with respect to the host lipids), these molecules are miscible with the host

Received for publication 14 December 1995 and in final form 11 April 1996.

Address reprint requests to Dr. André Lopez, Laboratoire de Pharmacologie et Toxicologie Fondamentales du CNRS, Department III, 118 Route de Narbonne, 31062 Toulouse Cedex, France. Tel.: 61-33-58-74; Fax: 61-33-58-86; E-mail: lopez@lptf.biotoul.fr.

0006-3495/96/07/327/09 $2.00

lipids when in the fluid phase. In this respect, the probe N-NBD-PE incorporated in lipids undergoing a gel-to-liquid phase transition has been reported as preferring the fluid phase, in both bilayers (Vaz et al., 1989) and monolayers (Peters and Beck, 1983; McConnell et al., 1984).

With respect to the fluorescence properties of the NBD group, two recent studies carried out on NBD derivatives in organic solvents have shown that this fluorophore exhibits solvatochromic properties because of the existence of a large dipole moment in the molecule that increases upon excitation (Fery-Forgues et al., 1993; Mukherjee et al., 1994). Changes in the polarity of the surrounding medium result mainly in changes in the quantum yield, dominated by the constant rate of the nonradiative deactivation processes (Fery-Forgues et al., 1993).

In most membrane studies with NBD-labeled phospholipids, it is implicitly assumed that the fluorescence response of the fluorophore does not depend on the chemical structure of the lipid to which it is attached and on the nature of the membrane in which the probe is inserted. In fact, biological membranes are complex multimolecular assemblies in which the environmental micropolarity can vary, depending on the protein and lipid composition. The NBD group is endowed with solvatochromic properties and is probably located in the water/membrane interfacial region, where the dielectric constant is known to vary abruptly from its value of ~80 in water to a value of ~2 in the hydrocarbon phase of the lipids (Brasseur et al., 1982; Tocanne and Teissié, 1990; Pérochon et al., 1992; Sanders and Schwonek, 1993). Subtle changes in the location of the fluorophore in this critical interfacial region due to changes in lipid and protein composition could have major consequences for its fluorescence response. For these reasons, the question of whether the fluorescence emission of NBD-labeled lipids depends on their own chemical structure and on that of the host membrane is to be considered, especially when these probes are used for investigating membrane organization and dynamics.

In this paper, by means of steady-state and time-resolved fluorescence experiments, we consider the behavior of a variety of NBD-labeled phospholipids embedded in various phospholipids. The main conclusion of this study is that the fluorescence properties of NBD-phospholipids depend on their own chemical structure and on that of the host lipids. A preliminary report of portions of this work has appeared previously (Mazères et al., 1995).

MATERIALS AND METHODS

Chemicals

All phospholipids were purchased from Sigma (St. Louis, MO), and the NBD-labeled phospholipids were obtained from Avanti Polar Lipids (Alabaster, AL). The purity of these compounds was checked by thin-layer chromatography on silica gel (Merck, Darmstadt, Germany) with the elution solvent chloroform/methanol/acetone/acetic acid/water (50:10:20:10:3 by volume). 7-Dimethylamino-3-(*p*-formylstyryl)-1,4-benzoxarine-2-one (DFSBO) was kindly provided by Dr. L. Cazaux (Laboratoire de Synthèse et Physicochimie Organique, Université P. Sabatier, Toulouse, France). Salts and solvents were of analytical grade. Chloroform solutions of phospholipids and NBD-labeled lipids were stored at 4°C. The concentration of lipid solutions was determined by phosphate assay subsequent to total digestion by perchloric acid (McClare, 1971).

Vesicle preparations

The desired NBD-phospholipid probe was added to a given phospholipid at a concentration of 2 mol% in chloroform solution. Chloroform was removed first by evaporation under nitrogen and then for at least 2 h under vacuum (1 torr). The dry lipid mixture was dispersed in a saline buffer (3-[*N*-morpholino]propanesulfonic acid 10 mM, pH 7, 100 mM NaCl, NaN_3 0.2%, mass by volume) at a final concentration of 0.5 10^{-3} M, then vortexed for 1 min and sonicated for 10 min with an immersed tip (50W Vibra-Cell; Bioblock Scientific, Strasbourg, France) at room temperature for egg yolk phosphatidylcholine (PC), phosphatidic acid from egg yolk phosphatidylcholine (PA), phosphatidylglycerol from egg yolk phosphatidylcholine (PG), and bovine brain phosphatidylserine (PS), and at a temperature 5°C above the gel-to-liquid phase transition temperature (T_m) for dimyristoylphosphatidylcholine (DMPC) and dipalmitoylphosphatidylcholine (DPPC). The small unilamellar vesicles thus obtained were kept overnight at 4°C. Vesicle-vesicle fusion occurred, which yielded, in equilibrium, completely relaxed unilamellar vesicles with an average diameter of about 80 nm (Nanosizer, model N4 MD; Coulter, Hialeah, FL). These lipid vesicles can be used within a few days. However, to prevent any chemical degradation of the fluorescent probes, these vesicles were used no more than 1 day after their preparation.

Spectroscopic measurements

Absorption spectra were measured with a Perking Elmer UV/VIS Lambda 16 spectrometer at 20°C (thermostated cuvette holder), using a 1-cm-path length quartz cuvette. The absorbance of vesicle suspensions was around 0.05 at 530 nm and never greater than 0.1 at 340 nm.

Emission spectra were recorded with an Aminco SPF 500 C spectrofluorometer interfaced with a PC microcomputer for storage, correction, and analysis of the data. Slit widths of 1 nm were used for all measurements. Fluorescence quantum yields ϕ were obtained by reference to DFSBO in ethanol (ϕ = 0.58; Le Bris et al., 1984). The experimental error in the determination of ϕ values was better than 2%. Refractive indexes were measured with a Carl Zeiss refractometer.

Fluorescence lifetime measurements

Fluorescence decays were monitored by a single photon counting technique. The excitation beam was produced by a picosecond mode-locked titanium/sapphire laser (Tsunami; Spectra Physics, Spectra Physics Lasers) tunable over a wavelength range of 700-1000 nm. The solid laser was pumped by an argon ion laser (BeamLok 2080; Spectra Physics) with a power beam adjustable from 7.5 W to 13 W. After the Tsunami, a pulse selector and a frequency doubler (model 3980; Spectra Physics) respectively enable the pulse repetition rate to be reduced from the nominal value of 82 MHz to lower values and the excitation wavelength to be selected between 349 nm and 420 nm. Experiments were carried out with a pulse repetition rate of 800 kHz and an excitation wavelength of 352 nm. Fluorescence was recorded at 530 nm with a monochromator (slit width: 2 nm) coupled to a Philipps 2020 photomultiplier tube. The remainder of the apparatus, which uses components of the spectrofluorimeter model 199 from Edinburgh Instrument (Edinburgh, Scotland), has been described elsewhere (Pérochon et al., 1992). The apparatus response function was evaluated by reference to the fluorescence decays of DFSBO in ethanol (τ = 2, 9 ns; Le Bris et al., 1984). Measurements were performed at 20°C in a thermostated cuvette. Decays were recorded over a time range of 50 ns and dispatched over the 1024 channels of the multichannel analyzer. After deconvolution of the apparatus response function, fluorescence decays

were analyzed as the sum of a finite number of exponentials using a least-squares algorithm, including a ponderation function accounting for the fact that the noise of photon counting obeys a Poisson law of distribution. Coupled with statistical analysis of the data, this procedure enabled us to calculate the characteristic time τ_i and the steady-state intensity I_i for each exponential entering a given fluorescence decay, according to the following equation:

$$I(t) = \sum_{i=1}^{i=n} I_i/\tau_i \exp(-t/\tau_i), \quad (1)$$

in which $I_i/\tau_i = \alpha_i$.

In the following, I_i and τ_i are given with an error risk of 5%, which corresponds on average to a variation of ±1% of solution values indicated in the tables.

RESULTS

Spectroscopic characteristics of NBD-labeled lipids in various phospholipids

Absorption spectra

The maximum absorption wavelengths λ_{π,π^*} and λ_{CT} (nm) of the π,π^* and charge transfer (CT) bands of the NBD group in liposomal dispersions of various NBD-labeled phospholipids embedded in various host phospholipids are shown in Table 1. These values cover a very narrow range around a central value of 335 nm for the π,π^* band and 470 nm for the CT band.

Fluorescence spectra

Fig. 1 shows the corrected fluorescence spectra recorded upon excitation of the above liposomal suspensions in the π,π^* band of the NBD group, after normalization with respect to the quantum yields (see Table 2). Table 1 shows the maximum fluorescence emission wavelengths λ_{em}^{max} upon excitation of the fluorophore in the π,π^* ($\lambda_{ex} \approx 336$ nm) or the charge transfer ($\lambda_{ex} \approx 470$ nm) bands. Whatever the lipid probe, the host phospholipids and the excitation wavelength remained nearly unchanged around a value of 541 ± 2 nm. A similar value of 535 nm has been reported by Chattopadhyay and London (1988) for N-NBD-PE, NBD(C_{12})-PC, and NBD(C_6)-PC in multilamellar vesicles of DOPC.

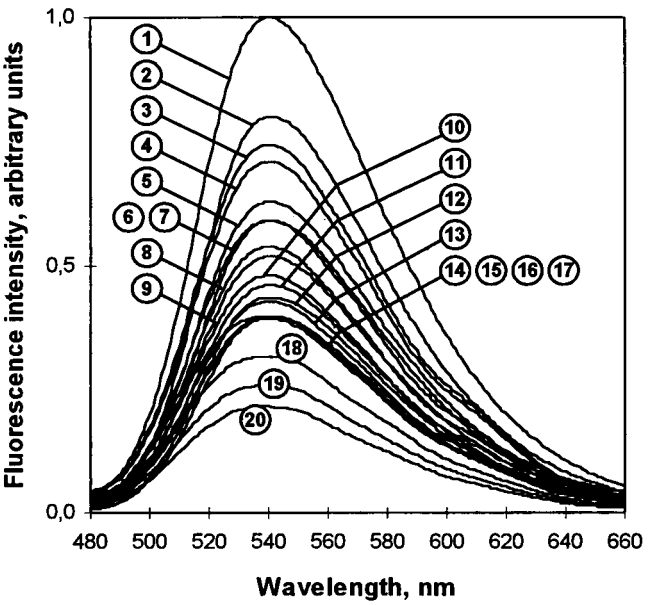

FIGURE 1 Corrected fluorescence emission spectra of NBD-labeled phospholipids inserted within various host phospholipids. 1: NBD(C_{12})-PE/PC; 2: NBD(C_{12})-PG/PC; 3: N-NBD-PE/PC; 4: NBD(C_{12})-PC/PC; 5: NBD(C_{12})-PE/PS; 6: NBD(C_{12})-PG/PS; 7: N-NBD-PE/PS; 8: N-NBD-PE/PA; 9: NBD(C_{12})-PE/PA; 10: NBD(C_{12})-PC/PS; 11: NBD(C_{12})-PE/PG; 12: NBD(C_{12})-PG/PA; 13: NBD(C_{12})-PC/PA; 14: NBD(C_{12})-PA/PC; 15: NBD(C_{12})-PG/PG; 16: N-NBD-PE/PG; 17: NBD(C_{12})-PC/PG; 18: NBD(C_{12})-PA/PS; 19: NBD(C_{12})-PA/PA; 20: NBD(C_{12})-PA/PG. Spectra were normalyzed with respect to the quantum yield. λ_{ex} was 352 nm.

The molar extinction coefficients of the π,π^* and CT bands of the NBD group have been reported, respectively, as being insensitive and very sensitive to the polarity of the surrounding medium (Fery-Forgues et al., 1993; Lancet and Pecht, 1977). For that reason, all of the fluorescence data reported in this study correspond to an excitation of the NBD fluorophore in the π,π^* band.

A red edge excitation shift (REES), i.e., a shift in the wavelength of maximum fluorescence emission toward higher wavelengths, caused by a shift in the excitation wavelength toward the red edge of the absorption band, can be observed for polar fluorophores in motionally restricted media (Chattopadhyay and Mukherjee, 1993). A REES of 10 nm from λ_{em}^{max} = 530 nm to λ_{em}^{max} = 540 nm was measured when illuminating N-NBD-PE/DOPC vesicles from 460 nm to 520 nm (Chattopadhyay and Mukherjee,

TABLE 1 Maximum absorption wavelengths λ_{π,π^*} and λ_{CT} (nm) of the π, π^* and charge transfer bands measured for liposomal dispersions of various NBD-labeled phospholipids embedded (2 mol%) in various host phospholipids

NBD-labeled lipids	Transition	Wavelength (nm) Host Lipids PC	PA	PG	PS
NBD(C_{12})-PC	π,π^*	336	339	337	336
	CT	471	472	470	473
	Fluorescence	541	542	542	540
NBD(C_{12})-PA	π,π^*	334	336	335	338
	CT	470	469	469	470
	Fluorescence	541	540	541	539
NBD(C_{12})-PG	π,π^*	334	337	334	336
	CT	470	471	470	471
	Fluorescence	541	543	542	541
NBD(C_{12})-PE	π,π^*	336	336	335	334
	CT	471	469	469	472
	Fluorescence	542	543	541	541
N-NBD-PE	π,π^*	333	335	332	335
	CT	466	463	469	465
	Fluorescence	540	543	540	540

Also shown are the maximum fluorescence emission wavelengths λ_{em} (nm) obtained upon excitation of the fluorophore in the π,π^* ($\lambda_{ex} \approx 336$ nm) or the charge transfer ($\lambda_{ex} \approx 470$ nm) bands.

TABLE 2 Fluorescence quantum yield ϕ and fluorescence lifetime τ (ns) obtained for liposomal dispersions of NBD-labeled phospholipids in various host phospholipids

NBD-labeled lipids	Host Lipids: PC ϕ	PC τ	PA ϕ	PA τ	PG ϕ	PG τ	PS ϕ	PS τ
NBD(C_{12})-PC	0.148	6.0	0.089	5.0	0.082	5.1	0.100	4.7
NBD(C_{12})-PA	0.083	6.0	0.054	5.5	0.045	5.6	0.066	4.9
NBD(C_{12})-PG	0.167	6.0	0.091	4.8	0.083	4.8	0.123	4.7
NBD(C_{12})-PE	0.209	5.7	0.108	4.4	0.096	4.8	0.131	4.3
NBD(C_6)-PE	0.191	⟨5.9⟩*	0.088	⟨4.7⟩#	0.073	⟨4.9⟩§	0.109	⟨4.5⟩¶
N-NBD-PE	0.155	7.9	0.112	6.2	0.083	6.4	0.123	5.4

With the exception of NBD(C_6)-PE, good fitting of the fluorescence decays was achieved with one exponential. The relative uncertainties were smaller, respectively, than 2% for ϕ and 1% for τ. For NBD(C_6)-PE, two exponentials were required: $^*\tau_1$ = 6.3 ns; I_1 = 92%; τ_2 = 1.2 ns; $^\#\tau_1$ = 6.3 ns; I_1 = 62%; τ_2 = 2.2 ns; $^\S\tau_1$ = 6.2 ns; I_1 = 68%; τ_2 = 2.1 ns; $^\P\tau_1$ = 5.7 ns; I_1 = 52%; τ_2 = 3.2 ns. The mean lifetime values shown in the table were calculated using the classical relation: $\langle\tau\rangle = (I_1\tau_1 + I_2\tau_2)/I_1 + I_2)$.

1993). This was taken as an argument suggesting that NBD-labeled lipids might serve to probe membrane organization and dynamics. In our hands, the same procedure over the same wavelength range yielded a REES of only ~4 nm for the same probe/lipid couple and a REES of ~3 nm for the other NBD-labeled lipids and host lipids tested in this study. However, lipid concentrations and slit widths used in the present study differed slightly from those described by Chattopadhyay and Mukherjee (1993). This might partly explain the observed differences in REES values.

Fluorescence quantum yields

As shown in Table 2 and Fig. 1, the fluorescence quantum yield of NBD-labeled lipids can vary by up to a factor of 4.6 when changing the chemical structure of the probes and that of the surrounding lipids. For a given host lipid, changes in ϕ with probe structure were rather complex. However, and as a genaral feature, the larger ϕ values were observed for NBD(C_{12})-PE and the lower ϕ values were observed for NBD(C_{12})-PA. By contrast, the influence of lipid environment on probe behavior was more regular. For each probe, ϕ was found to decrease in the order PC > PS > PA > PG.

Fluorescence lifetimes

With the exception of NBD(C_6)-PE, which required two exponentials, all of the fluorescence decays recorded for the various probes and host phospholipids tested were well fitted (χ^2 values < 2.0) with one exponential. As can be seen in Table 2, fluorescence lifetimes were distributed in a complex manner around a central value of ~5.3 ns. As a general trend, the highest τ values were found for the N-NBD-PE probe and for the PC host lipid.

From ϕ and τ values in Table 2, it is possible to calculate the corresponding radiative k_r and nonradiative k_{nr} rate constants of deactivation of the NBD group using the photophysical equations

$$k_r = \phi/\tau \tag{2}$$

$$k_{nr} = (1 - \phi)/\tau \tag{3}$$

Because of the uncertainty of τ and ϕ, k_r and k_{nr} were determined with a confidence level better than 95%. Results are shown in Table 3.

From inspection of the data, it turns out that deactivation of excited chromophores was dominated by the nonradiative process, with k_{nr}/k_r ratios of 8.5 on average. For each probe, the lowest k_{nr} values were found in PC. Irrespective of the

TABLE 3 Radiative (k_r, s^{-1}), and nonradiative (k_{nr}, s^{-1}) rate constants of deactivation obtained for liposomal dispersions of NBD-labeled phospholipids inserted in various host phospholipids

NBD-labeled lipids	Host Lipids: PC $k_{nr} \times 10^{-8}$	PC $k_r \times 10^{-8}$	PA $k_{nr} \times 10^{-8}$	PA $k_r \times 10^{-8}$	PG $k_{nr} \times 10^{-8}$	PG $k_r \times 10^{-8}$	PS $k_{nr} \times 10^{-8}$	PS $k_r \times 10^{-8}$
NBD(C_{12})-PC	1.42	0.25	1.82	0.18	1.80	0.16	1.91	0.21
NBD(C_{12})-PA	1.53	0.14	1.72	0.10	1.71	0.08	1.91	0.13
NBD(C_{12})-PG	1.39	0.28	1.89	0.19	1.91	0.17	1.87	0.26
NBD(C_{12})-PE	1.39	0.37	2.03	0.25	1.88	0.20	2.02	0.30
NBD(C_6)-PE	1.37	0.32	1.94	0.19	1.89	0.15	1.78	0.22
N-NBD-PE	1.07	0.20	1.43	0.18	1.43	0.13	1.62	0.23

The relative uncertainties for these parameters were around 3%.

host lipids, the highest and lowest k_r values were found for NBD(C_{12})-PE and NBD(C_{12})-PA, respectively, whereas for each lipid probe, k_r depended on the host lipids in decreasing order: PC > PS > PA > PG.

Spectroscopic characteristics of NBD-labeled lipids in DMPC and of NBD(C_{12})-PC in DPPC

To test the influence of lipid phase transition on the fluorescence properties of the lipid probes, and absorption and fluorescence spectra, fluorescence quantum yields and lifetimes of liposomal dispersions of the various NBD-labeled lipids inserted in DMPC were measured at various temperatures. ϕ and τ values are shown in Table 4. The corresponding k_r and k_{nr} constants are shown in Table 5 and plotted versus temperature in Fig. 2. As can be seen, k_r was not significantly affected by temperature, whereas k_{nr} was. Thus, a regular increase in k_{nr} with rising temperature was observed for the NBD(C_{12})-PA probe. For the other probes, k_{nr} showed a minimum at 20°C, near the gel-to-liquid phase transition temperature (~23°C) of DMPC. In any case, and within the limits of uncertainty of our experiments, ϕ, τ, k_r, and k_{nr} values measured at 20°C in DMPC were close to those obtained in PC for the same lipid probes and at the same temperature.

For the sake of comparison, these experiments were also perfomed with NBD(C12)-PC in DPPC. Corresponding ϕ, τ, k_r, and k_{nr} values are reported in Table 6 and plotted versus temperature in Fig. 3. In this case as well, k_r was not affected by temperature, whereas k_{nr} was, with a minimum around the T_m (~ 41°C) of the host lipid. For temperatures above 41°C, where DPPC is in the fluid phase, an Arrhenius plot of k_{nr} yielded an activation energy of 15 kJ/mol for the nonradiative deactivation process of NBD. This value is close to that of 17 kJ/mol found by Fery-Forgues et al. (1993) for *n*-propylamino-NBD in solution in benzene or in dimethylsulfoxide.

DISCUSSION

It is clear from the above data that the fluorescence properties of NBD-labeled phospholipids depend on the chemical structure and physical state of the host phospholipids and on their own chemical structure. Among the various fluorescence parameters studied, i.e., Stokes' shifts, lifetimes, and quantum yields, the latter was by far the most affected by these structural and environmental factors, whereas the former was practically unaffected. Thus, depending on the lipid probe and the host phospholipid, the fluorescence emission of the NBD group may vary in intensity by a factor of up to 4.6 (compare the quantum yield of NBD(C_{12})-PE in PC to that of NBD(C_{12})-PA in PG). In any case, ϕ is also affected by the phase state of the host lipids, with maximum values around the gel-to-liquid phase transition for lipids like DMPC and DPPC. In all cases, deexcitation of the fluorophore is dominated by the nonradiative process, with average k_{nr}/k_r ratios of 8.5.

Through steady-state and time-resolved fluorescence studies of various NBD derivatives (Fery-Forgues et al., 1993; Mukherjee et al., 1994), the NBD group has been shown to exhibit strong solvatochromic properties, which provides a clue to interpreting the above data. In particular, the quantum yield of *n*-propylamino-NBD (Fery-Forgues et al., 1993) appeared to be very sensitive to solvent polarity. These changes in ϕ were also dominated by the nonradiative constant k_{nr}. ϕ and k_{nr} values measured for this molecule in various organic solvents are plotted, respectively, in Figs. 4 and 5 versus the solvent dielectric constant ϵ. A ~25-fold decrease in ϕ and a ~25-fold increase in k_{nr} were observed when ϵ was increased from 2 to 78.5 (water). Because *n*-propylamino-NBD and NBD-labeled lipids are closely related chemically because of the NBD group, the former can be used as a reference for analyzing the influence of environmental polarity on the fluorescence response of the latter in comparison to diethylamino-NBD (Fery-Forgues et al., 1993). This analysis can be achieved with k_{nr}, which exhibits much more regular behavior than ϕ. Because of the great dependence of k_{nr} on ϵ, location of the NBD group where expected, i.e., in the aqueous phase for the headgroup-labeled lipid N-NBD-PE and in the hydrophobic core of the lipid bilayer for the acyl chain-labeled lipids, would result in quite different k_{nr} values for the two classes of lipid probes. At least for the acyl chain-labeled molecules, k_{nr} would be nearly independent of the nature of the host lipids. The contrary was observed, with a set of rather low, close k_{nr} values in the range 10^8 s^{-1} to 2×10^8 s^{-1},

TABLE 4 Influence of temperature on the fluorescence quantum yield ϕ and lifetime τ (ns) of NBD-labeled phospholipids inserted in DMPC liposomes

NBD-labeled lipids	DMPC							
	10°C		20°C		30°C		40°C	
	ϕ	τ	ϕ	τ	ϕ	τ	ϕ	τ
NBD(C_{12})-PC	0.122	5.0	0.147	5.5	0.139	5.2	0.112	4.3
NBD(C_{12})-PA	0.072	6.8	0.065	6.3	0.049	5.3	0.038	4.4
NBD(C_{12})-PG	0.116	4.9	0.138	5.2	0.135	5.1	0.098	4.3
NBD(C_{12})-PE	0.136	4.1	0.198	5.1	0.190	4.8	0.180	4.4
N-NBD-PE	0.117	7.8	0.125	7.9	0.120	7.4	0.105	6.1

The relative uncertainties were smaller, respectively, than 2% for ϕ and 1% for τ.

TABLE 5 Influence of temperature on the radiative (k_r, s^{-1}), and nonradiative (k_{nr}, s^{-1}) rate constants of deactivation of NBD-labeled phospholipids inserted in DMPC liposomes

NBD-labeled lipids	DMPC							
	10°C		20°C		30°C		40°C	
	$k_{nr} \times 10^{-8}$	$k_r \times 10^{-8}$	$k_{nr} \times 10^{-8}$	$k_r \times 10^{-8}$	$k_{nr} \times 10^{-8}$	$k_r \times 10^{-8}$	$k_{nr} \times 10^{-8}$	$k_r \times 10^{-8}$
NBD(C_{12})-PC	1.76	0.24	1.55	0.27	1.66	0.27	2.07	0.26
NBD(C_{12})-PA	1.36	0.11	1.48	0.10	1.77	0.09	2.19	0.09
NBD(C_{12})-PG	1.80	0.24	1.66	0.27	1.70	0.26	2.10	0.23
NBD(C_{12})-PE	1.88	0.33	1.57	0.39	1.69	0.40	1.86	0.41
N-NBD-PE	1.13	0.15	1.11	0.16	1.19	0.16	1.47	0.17

The relative uncertainties for these two parameters were around 3%.

which varied from one lipid to the other. According to the polarity scale of Figs. 4 and 5, these k_{nr} values account for a local dielectric constant of around 27–41, indicating that the NBD group was located in a region of the lipid bilayer of relatively high polarity. As already mentioned in the Introduction, this corresponds to the region of the lipid polar headgroups where an abrupt polarity gradient takes place. A similar conclusion was reached by Chattopadhyay and London (1987) for the probes N-NBD-PE and NBD(C_{12})-PC or NBD(C_6)-PC inserted in DOPC, using spin-label quenching experiments. The NBD group was found at distances of 14.2 Å and 12.2 Å from the bilayer center for the polar headgroup-labeled and acyl chain-labeled lipids, respectively. According to the authors, this would place the chromophore in the region of the glycerol backbone-carbonyl residues of the host phosphatidylcholine molecules.

Location in depth of the NBD group can also be estimated from our fluorescence data. Various models have been proposed to account for the polarity gradient that exists at water-lipid interfaces (Brasseur et al., 1982; Ram et al., 1992; Sanders and Schwonek, 1993). These models differ in their formulation and consequently in the final position and profile of the polarity gradient. We used the model suggested by Sanders and Schwonek (1993), which seems rather realistic and which was developed and successfully used to account for solute interactions with a water-phosphatidylcholine interface. In this model, based on the distribution function of water molecules in hydrated DOPC bilayers obtained by Wiener and White (1992) from x-ray and electron diffraction data, ϵ is assumed to vary from 78.5 in water to 2 in the hydrocarbon core of the lipid. Both the exponential shape of the transition function and the width of the dielectric transition are chosen, taking the experimental z-dependent variation in interfacial water concentration to be proportional to the local dielectric constant. These changes in ϵ along the bilayer normal are shown in Fig. 6, together with the distribution functions of the water molecules and the choline, phosphate, glycerol, and carbonyl

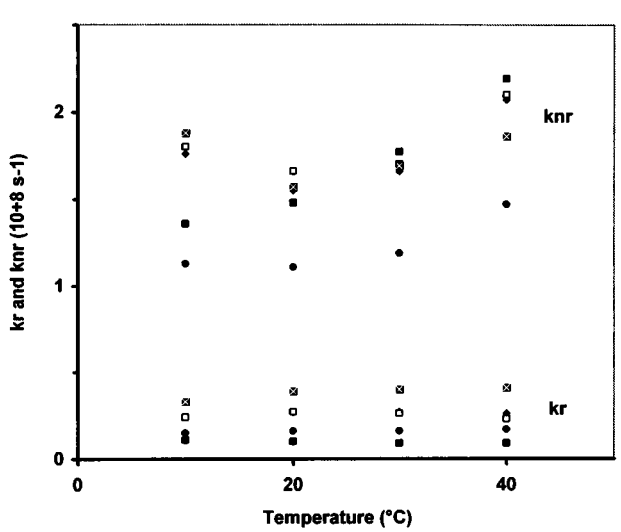

FIGURE 2 Influence of temperature on the nonradiative k_{nr} and radiative k_r deactivation rate constants of NBD(C_{12})-PE (⊠), NBD(C_{12})-PG (□), N-NBD-PE (●), NBD(C_{12})-PC (◆), and NBD(C_{12})-PA (■) in DMPC.

TABLE 6 Influence of temperature on the fluorescence quantum yield ϕ, lifetime τ (ns), and radiative (k_r, s^{-1}) and nonradiative (k_{nr} s^{-1}) rate constants of NBD(C_{12})-PC inserted in DPPC liposomes

Temperature (°C)	DPPC			
	ϕ	τ	$k_{nr} \times 10^{-8}$	$k_r \times 10^{-8}$
10	0.068	3.5	2.66	0.19
20	0.076	3.8	2.43	0.20
24	0.089	4.0	2.28	0.22
28	0.095	4.4	2.06	0.21
32	0.102	n.d.		
36	0.106	4.9	1.82	0.21
38	0.121	n.d.		
39	0.141	n.d.		
40	0.152	5.2	1.63	0.29
41	0.158	n.d.		
42	0.155	n.d.		
43	0.154	n.d.		
44	0.153	n.d.		
45	0.151	5.1	1.66	0.30
46	0.145	n.d.		
48	0.142	n.d.		
50	0.138	4.0	1.80	0.29
52	0.129	n.d.		
54	0.126	4.5	1.94	0.28
56	0.117	n.d.		
60	0.113	4.2	2.11	0.27

The relative uncertainties were smaller, respectively, than 2% for ϕ, 1% for τ, and 3% for k_{nr} and k_r.

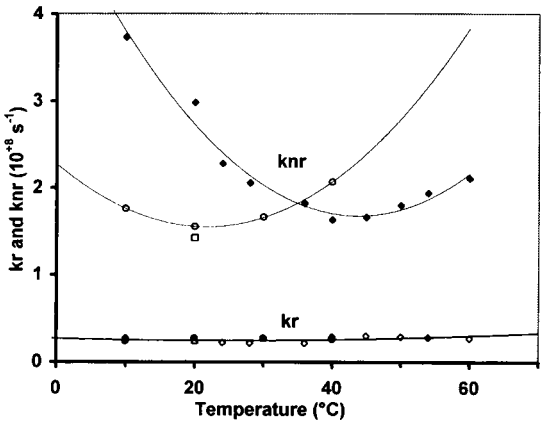

FIGURE 3 Influence of temperature on the nonradiative k_{nr} and radiative k_r deactivation rate constants of NBD(C_{12})-PC in DMPC (○), DPPC (◆), and PC (□).

moieties of phosphatidylcholine. In PC, acyl chain-labeled lipids exhibited k_{nr} values of 1.42×10^8 s^{-1} on average. From Figs. 4 and 5, this corresponds to a local dielectric constant of ~34, which places the NBD group in the phosphate-glycerol backbone region of the lipid (Fig. 6). With a k_{nr} value of 1.07×10^8 s^{-1} and therefore a ϵ value of ~27, the NBD group in N-NBD-PE would explore a slightly more hydrophobic environment, around the glycerol part of the lipid. These conclusions are slightly at variance with

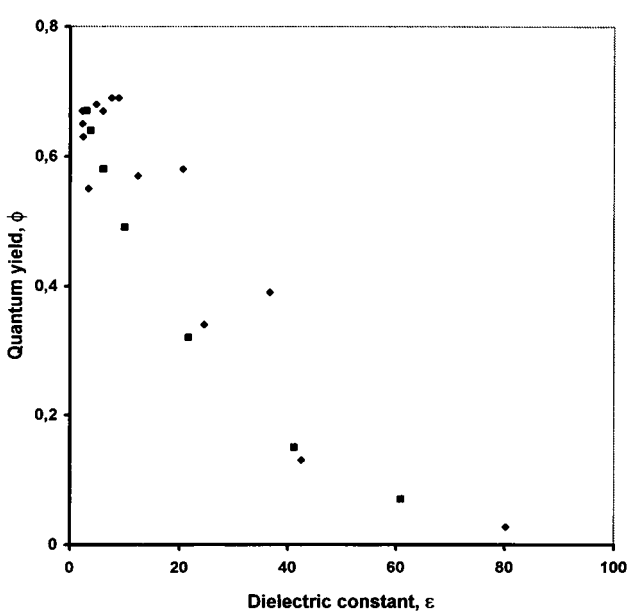

FIGURE 4 Plot of the fluorescence quantum yield ϕ of *n*-propylamino-NBD in organic solvents (◆) and water/dioxane mixtures (■) versus the solvent dielectric constant ϵ (taken from Fery-Forgues et al., 1993). The solvents used (with their dielectric constant; Riddick and Bunger, 1970) were trichloroethylene (3.42), toluene (2.38), ethyl acetate (6.02), 1,4-dioxane (2.21), tetrahydrofuran (7.58), benzene (2.27), acetone (20.70), acetonitrile (37.5), chloroform (4.81), methylene chloride (8.93), pyridine (12.4), dimethylformamide (36.71), dimethylsulfoxide (46.68), ethanol (24.55), glycerol (42.5), and water (80.20).

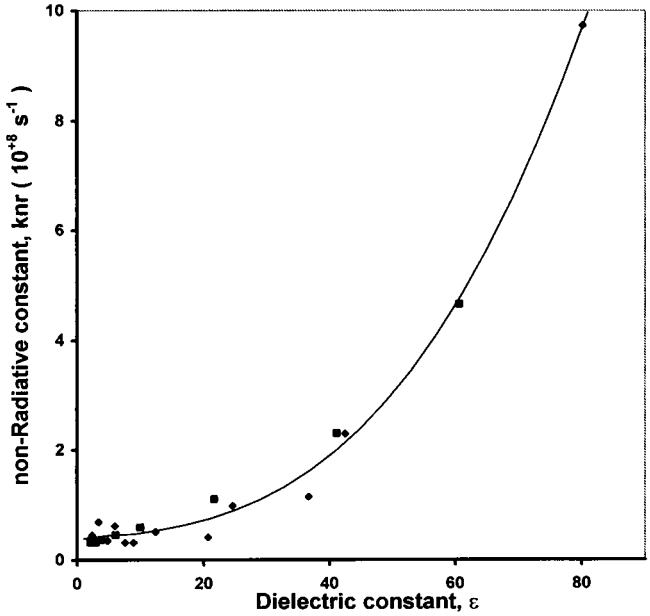

FIGURE 5 Plot of the nonradiative deactivation rate constant k_{nr} of *n*-propylamino-NBD in organic solvents (◆) and water/dioxane mixtures (■) versus the solvent dielectric constant ϵ (taken from Fery-Forgues et al., 1993). For solvents used see Fig. 4.

those of Chattopadhyay and London (1987), which, for the same couple of labeled and host lipids, placed the chromophore in a more hydrophobic environment. Note that when the distribution functions in Fig. 6 are used, the distances from the bilayer center of ~12 Å for NBD(C_{12})-PC and ~14 Å for N-NBD-PE found by Chattopadhyay and London (1987) would in fact place the NBD group in an even more hydrophobic environment, at the beginning of the hydrocarbon chain region. Our fluorescence data clearly account for a strongly polar environment, i.e., the water-lipid interface. They are in agreement with the more accurate results of Abrams and London (1993), which locate the NBD group of N-NBD-PE and NBD(C_{12})-PC at distances of 18.9 and 19.8 Å, respectively, from the center of the bilayer. Our study also clearly indicates that the NBD group NBD(C_{12})-PC is in a more polar environment than N-NBD-PE, with k_{nr} values of 1.42×10^8 s^{-1} and 1.07×10^8 s^{-1}, respectively. In this respect, it is worth noting that the k_{nr} value of 2.66×10^8 s^{-1} measured for NBD(C_{12})-PC in DPPC at 10°C, compared with the k_{nr} value of 1.66×10^8 s^{-1} at 40°C, suggests that, in the gel phase and as compared to the fluid phase, the NBD group is expelled from the bilayer toward the aqueous phase and now explores the highly polar phosphocholine region of the water-lipid interface.

In PA, PG, and PS, k_{nr} values of around 1.5×10^8 s^{-1} for N-NBD-PE and 1.9×10^8 s^{-1} for the acyl chain-labeled lipids correspond to local dielectric constants of 35 and 41, respectively. The distribution functions of the water and constitutive groups of these phospholipids and the profiles of the corresponding interfacial polarity gradients have not

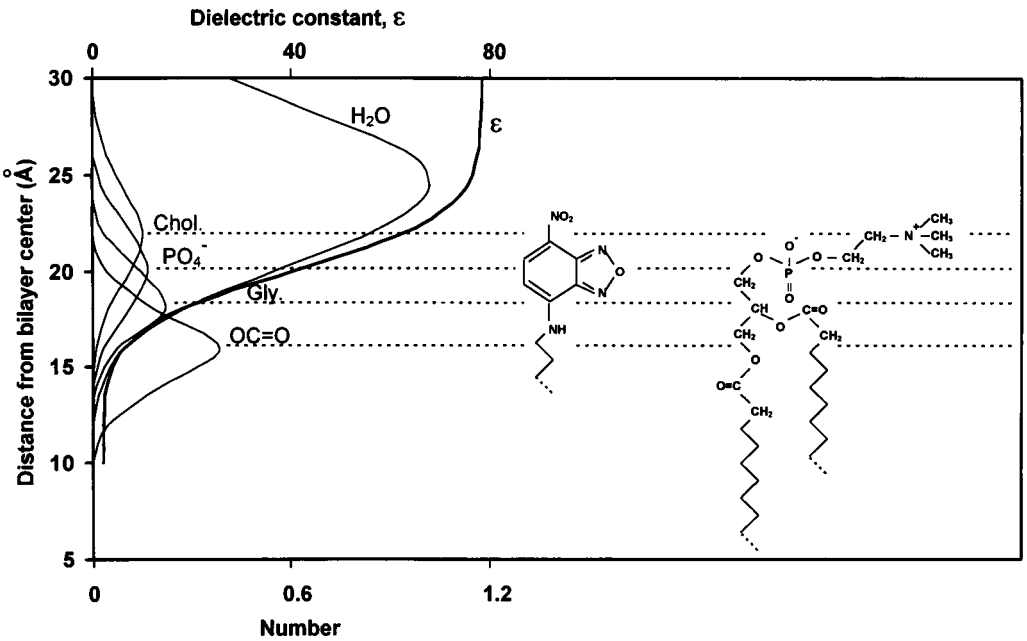

FIGURE 6 Schematic representation of the localization of the NBD group for acyl chain-labeled phospholipids inserted in egg yolk phosphatidylcholine bilayers. Also shown are the distribution functions (Number) of the water and choline (Chol.), phosphate (PO_4), glycerol (Gly.), and carbonyl (OC═O) moieties of the host phospholipid and the dielectric constant (ϵ), plotted against the distance from the bilayer center ($z = 0$). The distribution functions were taken from Wiener and White (1992), and changes in ϵ were calculated from Sanders and Schwonek (1993). The position of the NBD group accounts for a local dielectric constant of 34 deduced (see Fig. 5) from a nonradiative deactivation rate constant value of $1.42 \times 10^8\ s^{-1}$ (average of the k_{nr} values measured for NBD(C_{12})-PE, NBD(C_{12})-PC, NBD(C_{12})-PA, and NBD(C_{12})-PG in PC).

been determined. However, one can reasonably assume that these structural parameters do not differ very much from one phospholipid to the other and that in PA, PG, and PS, as in PC, the NBD group is located in the region of the polar headgroups.

As previously discussed (Chattopadhyay and London, 1987; Chattopadhyay, 1990), location of the NBD group at the water-lipid interface results from a looping back from the bilayer center toward the surface, because of the high polarity of this chromophore and is permitted by the flexibility of the acyl chains. In this view, the NBD group should adopt different orientations when entering the interface, either from the aqueous phase or from the bilayer center. This would explain the systematic differences in polarity detected by the headgroup-labeled N-NBD-PE as compared to the acyl chain-labeled phospholipids.

Altogether, NBD-labeled phospholipids display complex fluorescence properties that may be difficult to analyze, especially in natural membranes. In particular, the great sensitivity of the probe quantum yield to environmental factors will make any attempt to use fluorescence intensity for quantifying probe concentrations in membranes doubtful. On the other hand, this remarkable propensity of NBD-labeled lipids to probe the polarity of their environment would make these molecules well suited to the investigation of membrane organization and the detection of membrane domains.

We thank John Robb for reading the English manuscript.

REFERENCES

Abrams, F. S., and E. London. 1993. Extension of the parallax analysis of membrane penetration depth to the polar region of model membranes: use of fluorescence quenching by a spin-label attached to the phospholipid polar headgroup. *Biochemistry.* 32:10826–10831.

Bacallao, R., C. Antony, C. Dotti, E. Karsenti, E. H. K. Stelzer, and K. Simons. 1989. The subcellular organization of Madin-Darby canine kidney cells during the formation of a polarized epithelium. *J. Cell Biol.* 109:2817–2832.

Brasseur, R., M. Deleers, W. J. Malaisse, and J. M. Ruysschaert. 1982. Conformational analysis of the calcium-A23187 complex at a lipid-water interface. *Proc. Natl. Acad. Sci. USA.* 79:2895–2897.

Chattopadhyay, A. 1990. Chemistry and biology of *N*-(7-nitrobenz-2-oxa-1,3-diazol-4-yl)-labeled lipids: fluorescent probes of biological and model membranes. *Chem. Phys. Lipids.* 53:1–15.

Chattopadhyay, A., and E. London. 1987. Parallax method for direct measurement of biomembrane penetration depth utilizing fluorescence quenching by spin-labeled phospholipids. *Biochemistry.* 26:39–45.

Chattopadhyay, A., and E. London. 1988. Spectroscopic and ionisation properties of *N*-(7-nitrobenz-2-oxa-1,3-diazol-4-yl)-labeled lipids in model membranes. *Biochim. Biophys. Acta.* 938:24–34.

Chattopadhyay, A., and S. Mukherjee. 1993. Fluorophore environments in membrane-bound probes: a red edge excitation shift study. *Biochemistry.* 32:3804–3811.

Devaux, P. F. 1991. Static and dynamic lipid asymmetry in cell membranes. *Biochemistry.* 30:1163–1173.

Edidin, M. 1993. Patches and fences: probing for plasma membrane domains. *J. Cell Sci.* 17:165–169.

Ellens, H., J. Bentz, and F. C. Szoka. 1986. Fusion of phosphatidylethanolamine-containing liposomes and mechanism of the L_α-H_{II} phase transition. *Biochemistry.* 25:4141–4147.

Fery-Forgues, S., J. P. Fayet, and A. Lopez. 1993. Drastic changes in the fluorescence properties of NBD probes with the polarity of the medium: involvement of TICT state? *Photochem. Photobiol. A Chem.* 70: 229–243.

Ghosh, P. B., and M. W. Whitehouse. 1968. 7-Chloro-4-nitrobenzo-2-1,3-diazole: a new fluorigenic reagent for amino acids and other amines. *Biochem. J.* 108:155–163.

Hong, K., P. A. Baldwin, T. M. Allen, and D. Papahadjopoulos. 1988. Fluorometric detection of the bilayer-to-hexagonal phase transition in liposomes. *Biochemistry.* 27:3947–3955.

Julien, M., J. F. Tournier, and J. F. Tocanne. 1993. Differences in the transbilayer and lateral motions of fluorescent analogs of phosphatidylcholine and phosphatidylethanolamine in the apical plasma membrane of bovine aortic endothelial cells. *Exp. Cell Res.* 208:387–397.

Lancet, D., and I. Pecht. 1977. Spectroscopic and immunochemical studies with nitrobenoxadiazolealanine, a fluorescent dinitrophenyl analogue. *Biochemistry.* 16:5150–5157.

Le Bris, M. T., J. Mugnier, J. Bourson, and B. Valeur. 1984. Spectral properties of a new fluorescent dye emitting in the red: a benzoxazinone derivative. *Chem. Phys. Lett.* 106:124–127.

Mazères, S., V. Schram, S. Fery-Forgues, J.-F. Tocanne, and A. Lopez. 1995. Fluorescence properties of NBD-labeled phospholipids in membranes. *Biophys. J.* 68:A303.

McClare, C. W. F. 1971. An accurate and convenient organic phosphorus assay. *Anal. Biochem.* 39:527–530.

McConnell, H. M., L. K. Tamm, and R. M. Weis. 1984. Periodic structures in lipid monolayer phase transitions. *Proc. Natl. Acad. Sci. USA.* 81: 3249–3253.

Mukherjee, S., A. Chattopadhyay, A. Samata, and T. Soujanya. 1994. Dipole moment change of NBD group upon excitation studied using solvatochromic and quantum chemical approaches: implications in membrane research. *J. Phys. Chem.* 98:2809–2812.

Pagano, R. E., and O. C. Martin. 1988. A series of fluorescent *N*-acylsphingosines: synthesis, physical properties, and studies in cultured cells. *Biochemistry.* 27:4439–4445.

Pagano, R. E., and R. G. Sleight. 1985. Defining lipid transport pathaways in animal cells. *Science.* 229:1051–1057.

Pérochon, E., A. Lopez, and J. F. Tocanne. 1992. Polarity of lipid bilayers. A fluorescence investigation. *Biochemistry.* 31:7672–7682.

Peters, R., and K. Beck. 1983. Translational diffusion in phospholipid monolayers measured by fluorescence microphotolysis. *Proc. Natl. Acad. Sci. USA.* 80:713–7187.

Ram, P., E. Kim, D. S. Thomson, K. P. Howard, and J. H. Prestegard. 1992. Computer modelling of glycolipids at membrane surfaces. *Biophys. J.* 63:1530–1535.

Riddick, J. A., and W. B. Bunger. 1970. Physical properties tabulations. *In* Organic Solvents: Physical Properties and Method of Purification. John Wiley and Sons, New York. 66–501.

Sanders, C. R., II, and J. P. Schwonek. 1993. An approximate model and empirical energy function for solute interactions with a water-phosphatidylcholine interface. *Biophys. J.* 65:1207–1218.

Schram, V., J. F. Tocanne, and A. Lopez. 1994. Influence of obstacles on lipid lateral diffusion: computer simulation of FRAP experiments and application to proteoliposomes and biomembranes. *Eur. Biophys. J.* 23:337–348.

Stuck, D. K., D. Hoekstra, and R. E. Pagano. 1981. Use of resonance energy transfer to monitor membrane fusion. *Biochemistry.* 20: 4093–4099.

Tocanne, J. F., L. Dupou-Cezanne, and A. Lopez. 1994. Lateral diffusion of lipids in model and natural membranes. *Prog. Lipid Res.* 33:203–237.

Tocanne, J. F., and J. Tessié. 1990. Ionization of phospholipids and phospholipolid-supported interfacial lateral diffusion of protons in membrane model systels. *Biochim. Biophys. Acta.* 1031:111–142.

Vaz, W. L. C., E. C. C. Melo, and T. E. Thompson. 1989. Translational diffusion and fluid connectivity in a two-component, two phase phospholipid bilayer. *Biophys. J.* 56:869–876.

Welti, R., and M. Glaser. 1994. Lipid domains in model and biological membranes. *Chem. Phys. Lipids.* 73:121–137.

Wiener, M. C., and S. H. White. 1992. Structure of a fluid dioleoylphosphatidylcholine bilayer determined by joint refinement of x-ray and neutron diffraction data. III. Complete structure. *Biophys. J.* 61: 434–447.